


## SUPPLEMENTARY MATERIAL

### Detailed methods and techniques for calculating water yields using the InVEST model

Jaka Suryanta\*<sup>1)</sup> , Irmadi Nahib<sup>1)</sup> , Fadhlullah Ramadhani<sup>1)</sup> ,  
Farid Rifaie<sup>1)</sup> , Nawa Suwedi<sup>1)</sup> , Vicca Karolinoerita<sup>1)</sup> ,  
Destika Cahyana<sup>2)</sup> , Fahmi Amhar<sup>1)</sup> , Suprajaka<sup>3)</sup> 

<sup>1)</sup> Research Center for Geospatial, National Research and Innovation Agency of Indonesia (BRIN), Jalan Raya Jakarta Bogor KM 47 Cibinong, Bogor, West Java 16911, Indonesia

<sup>2)</sup> Research Center for Food Crops, Research Organization for Agriculture and Food, Jalan Raya Jakarta-Bogor Km. 46, Cibinong, Bogor, West Java 16911, Indonesia

<sup>3)</sup> Center for Research, Promotion and Cooperation, Geospatial Information Agency, Jalan Raya Jakarta-Bogor Km. 46, Cibinong, Bogor, West Java 16911, Indonesia

\* Corresponding author

The hydrological analysis method in ArcGIS uses DEM data, possessed with an 8-meter resolution as input, and providing the output applicable to many sub-watersheds (BIG, 2021). The Central Citarum watershed is currently divided into 17 sub-watersheds, and the names correspond to the ID of the Citarum watershed management. Then, this research has generated a 20-year precipitation map by utilising data from six meteorological, climatological, and geophysical stations, specifically focusing on rainfall measurements in 2006–2018.

Kriging interpolation is utilised to create annual and monthly average rainfall maps. Annual and monthly evapotranspiration maps were acquired and cropped according to the research region (CGIAR, 2019).

Subsequently, another stage encompasses the mapping of plant water content and soil solum depth by integrating soil maps sourced from Sulaeman *et al.* (2013) with HWSO soil texture data (FAO, 2022). Based on the land cover map, a biophysical table and a water demand table were created. After that, each layer produced from the land cover map was converted to a raster format with a resolution of 30×30 m. These maps, together with the shapefile of the sub-watershed, were fed into the InVEST model. As the model's output, the program provides a map depicting the water yield and consumption for each sub-watershed.

The water balance model (Gan, Liu and Sun, 2021) and the mean annual average rainfall determine the water balance principles. The InVEST model, according to the research flowchart, requires specified data inputs. Tallis *et al.* (2011) used Equation (S1) to determine the yearly processed data for each pixel, represented as  $Y_{(x)}$ , relating to a certain land cover. In this InVEST model, the quantity of water flowing from the landscape is referred to as water yield, with average water volumes and yields calculated using sub-catchment-level water balancing principles (Gerstorf and Schupp (eds.), 2016). Water balance principles are established using the Budyko water balance model and the yearly average rainfall. Nugroho (2022) introduced Equation (S1) to compute yearly water yield data for each pixel, expressed as  $Y(x)$ , associated with a certain land cover category.

The annual  $WY$  for a given land use and land cover (LULC) at each pixel,  $Y_{(x)}$ , was set as follows:

$$Y_{(x)} = \left(1 - \frac{AET_{(x)}}{P_{(x)}}\right) P_{(x)} \quad (S1)$$

where:  $AET_{(x)}$  = observed annual evapotranspiration at the specific pixel  $x$ ,  $P_{(x)}$  = yearly precipitation at the specific pixel  $x$ .

For LULC that has been vegetated (Fu, 1981),  $\frac{AET_{(x)}}{P_{(x)}}$  is the estimation of yearly precipitation on pixel  $x$  done in a spatially explicit way:

$$\frac{AET_{(x)}}{P_{(x)}} = 1 + \frac{PET_{(x)}}{P_{(x)}} - \left[1 + \left(\frac{PET_{(x)}}{P_{(x)}}\right)^\omega\right]^{\frac{1}{\omega}} \quad (S2)$$

where:  $PET_{(x)}$  = pixel  $x$ 's potential evapotranspiration,  $\omega$  = non-physical characteristics that define the relationship between climate and soil conditions, often known as the coefficient of available water capacity for plants.

To determine possible evapotranspiration,  $PET_{(x)}$ , Equation (S2) was used:

$$PET_{(x)} = ETO_{(x)} Kc_{(x)} \quad (S3)$$

where:  $ETO_{(x)}$  = reference evapotranspiration at the specified pixel  $x$ ,  $Kc_{(x)}$  = vegetation evapotranspiration coefficient at pixel  $x$ , which is related to its LULC categorisation (Zhang *et al.*, 2004).

The plant's available water capacity coefficient at each pixel, denoted as  $\omega_{(x)}$  as calculated using the approach presented by (Sánchez-Canales *et al.*, 2012) given by Equation (S4):

$$\omega_{(x)} = Z \frac{AWC_{(x)}}{P_{(x)}} + 1.25 \quad (S4)$$

where:  $AWC_{(x)}$  = volume of available water capacity for the plant at each pixel (mm),  $Z$  = seasonality factor, also known as the Zhang coefficient, is an empirical constant that accounts for local precipitation patterns as well as other hydrogeological parameters.

In this study, a  $Z$  value of 4 was used, as recommended by Hamel and Guswa (2015) for tropical watersheds. This section includes both physical and non-physical characteristics of natural soil features in connection to climate. The available water capacity of soil refers to its ability to hold water that plants can use. It is represented as the  $AWC_{(x)}$  where  $(x)$  denotes the specific pixel or location (Hamel and Guswa, 2015). This metric is calculated using the plant available water capacity ( $PAWC$ ), minimum depth of the root limiting layer ( $Root1$ ), and the vegetation's root depth ( $Root2$ ). The following approach is used to perform the calculation:

$$AWC_{(x)} = \min(Root1, Root2) \cdot PAWC \quad (S5)$$

The evapotranspiration of reference plants  $ETO_{(x)}$  in the particular location reflects the local meteorological conditions, whereas  $Kc_{(x)}$  is influenced mostly by the land use and plant cover features unique to each pixel.

The actual evapotranspiration ( $AET$ ) in non-vegetated LULC regions, such as water bodies or settlements, is directly calculated based on the reference evapotranspiration. The quantity of rainfall determines the upper limit of  $ETO_{(x)}$ , and the estimate approach is as follows:

$$AET_{(x)} = \min(Kc_{(x)} \cdot ETO_{(x)}, P_{(x)}) \quad (S6)$$

The modified Hargreaves equation (BIG, 2015) was used to compute reference evapotranspiration,  $ETo_{(x)}$  ( $\text{mm}\cdot\text{d}^{-1}$ ). When the following data are provided, this method is thought to produce more accurate findings than Penman–Monteith method:

$$ETo_{(x)} = 0.0013 \cdot 0.408Ra \left[ \left( \frac{T_{\max} + T_{\min}}{2} \right) + 17 \right] [(T_{\max} - T_{\min}) - 0.0123P]^{0.76} \quad (S7)$$

where:  $Ra$  = extra-terrestrial solar radiation ( $\text{MJ}\cdot\text{m}^{-2}\cdot\text{d}^{-1}$ ),  $T_{\max}$  = average maximum daily air temperature ( $^{\circ}\text{C}$ ),  $T_{\min}$  = average minimum daily air temperature ( $^{\circ}\text{C}$ ),  $P$  = monthly precipitation ( $\text{mm}\cdot\text{d}^{-1}$ ).

The InVEST model validity was assessed by comparing it to the whole Wyoming dataset received from Liu *et al.* (2017). Linear regression analysis was used to compare the observed data to the estimated data generated by the model. Several statistical analyses were performed using the R program during the model validation phase depending on the study findings. The determination coefficient ( $R^2$ ), Pearson correlation ( $r$ ), and root mean square error ( $RMSE$ ) were all calculated as part of these investigations.

**Table S1.** Water supply ( $WS$ ), water demand ( $WD$ ), and water scarcity index ( $WSI$ ) in 2006 and 2018 based on sub-districts in the Central Citarum watershed

No	Sub-district	2006				2018			
		$WS$ $\cdot 10^9 \text{ m}^3$	$WD$ $\cdot 10^9 \text{ m}^3$	$SDR$	$WSI$	$WS$ $\cdot 10^9 \text{ m}^3$	$WD$ $\cdot 10^9 \text{ m}^3$	$SDR$	$WSI$
1	Sukanagara	1,978	1,470	1.35	0.13	1,666	1,911	0.87	(0.06)
2	Cilaku	98,023	21,349	4.59	0.66	108,428	27,803	3.90	0.59
3	Ngamprah	14,664	6,779	2.16	0.34	9,911	9,068	1.09	0.04
4	Sukabumi	377	57	6.62	0.82	255	74	3.45	0.54
5	Cianjur	44,095	15,254	2.89	0.46	45,954	19,842	2.32	0.36
6	Cisarua	57,811	22,885	2.53	0.40	38,792	33,255	1.17	0.07
7	Cipeundeuy	0	0	1.10	0.04	0	0	0.22	(0.66)
8	Cugenang	144,834	47,355	3.06	0.49	137,924	54,021	2.55	0.41
9	Kadudampit	525	55	9.52	0.98	441	76	5.82	0.76
10	Karang Tengah	70,475	23,263	3.03	0.48	77,927	30,276	2.57	0.41
11	Cikalong Wetan	247,694	72,293	3.43	0.53	160,022	96,877	1.65	0.22
12	Cisarua	3,763	436	8.64	0.94	3,185	566	5.63	0.75
13	Bojong	15,021	4,137	3.63	0.56	8,726	5,381	1.62	0.21
14	Tegalwaru	167,995	32,389	5.19	0.71	143,506	42,116	3.41	0.53
15	Tanjungsari	198	87	2.26	0.35	184	114	1.62	0.21
16	Rancabali	381	61	6.19	0.79	336	120	2.81	0.45
17	Ciwidey	902	294	3.07	0.49	843	425	1.98	0.30
18	Sindangkerta	43,805	14,914	2.94	0.47	37,928	21,309	1.78	0.25
19	Cipongkor	943	317	2.97	0.47	812	415	1.96	0.29
20	Cibeber	249,597	68,222	3.66	0.56	266,220	89,171	2.99	0.48
21	Saguling	62	46	1.36	0.13	25	65	0.39	(0.41)
22	Bojong Picung	116,680	34,770	3.36	0.53	130,149	45,283	2.87	0.46
23	Gekbrong	90,609	27,979	3.24	0.51	92,269	34,759	2.65	0.42
24	Warung Kondang	93,091	28,644	3.25	0.51	94,760	34,860	2.72	0.43
25	Haurwangi	44,662	23,885	1.87	0.27	49,021	31,305	1.57	0.19

No	Sub-district	2006				2018			
		<i>WS</i> ·10 <sup>9</sup> m <sup>3</sup>	<i>WD</i> ·10 <sup>9</sup> m <sup>3</sup>	<i>SDR</i>	<i>WSI</i>	<i>WS</i> ·10 <sup>9</sup> m <sup>3</sup>	<i>WD</i> ·10 <sup>9</sup> m <sup>3</sup>	<i>SDR</i>	<i>WSI</i>
26	Padalarang	24,326	9,763	2.49	0.40	17,276	12,774	1.35	0.13
27	Cipatat	131,722	63,505	2.07	0.32	112,444	84,572	1.33	0.12
28	Sukaluyu	70,907	18,662	3.80	0.58	81,678	24,304	3.36	0.53
29	Ciranjang	38,117	15,058	2.53	0.40	44,233	19,633	2.25	0.35
30	Mande	122,075	61,742	1.98	0.30	114,871	79,220	1.45	0.16
31	Pacet	72,166	19,817	3.64	0.56	61,294	28,914	2.12	0.33
32	Cipeundeuy	137,854	59,086	2.33	0.37	112,033	77,431	1.45	0.16
33	Pacet	10,120	3,768	2.69	0.43	7,956	6,435	1.24	0.09
34	Sukaresmi	89,540	30,110	2.97	0.47	77,584	45,667	1.70	0.23
35	Pacet	95,426	27,280	3.50	0.54	74,492	37,306	2.00	0.30
36	Darangdan	134,636	30,889	4.36	0.64	85,083	40,193	2.12	0.33
37	Manis	107,632	55,281	1.95	0.29	93,750	71,811	1.31	0.12
38	Plered	90,501	18,911	4.79	0.68	66,935	24,604	2.72	0.43
39	Cikalong Kulon	164,204	89,533	1.83	0.26	152,504	121,601	1.25	0.10
40	Sukasari	433,160	88,222	4.91	0.69	347,981	114,107	3.05	0.48
41	Pagelaran	1,790	333	5.37	0.73	1,367	447	3.06	0.49
42	Campaka Mulya	154,593	27,048	5.72	0.76	123,796	39,097	3.17	0.50
43	Gununghalu	217,161	55,268	3.93	0.59	170,530	74,164	2.30	0.36
44	Campaka	259,566	77,604	3.34	0.52	254,591	102,786	2.48	0.39
45	Cireunghas	14	9	1.51	0.18	14	12	1.22	0.09
46	Rongga	136,699	30,395	4.50	0.65	125,463	39,561	3.17	0.50
47	Sukalarang	469	80	5.85	0.77	368	104	3.53	0.55
48	Sukaraja	397	43	9.21	0.96	394	56	7.03	0.85
49	Sukatani	70,088	13,167	5.32	0.73	48,242	17,139	2.81	0.45
50	Jatiluhur	13,405	3,359	3.99	0.60	8,487	4,292	1.98	0.30
51	Tegal Waru	75	9	8.34	0.92	74	12	6.37	0.80
52	Telukjambe Barat	80	20	3.95	0.60	63	27	2.32	0.37

Explanations: *WS* = water supply, *SDR* = supply-demand ratio.

Source: own study.

## REFERENCES

- BIG (2021) *DEMNAS*. Available at: <https://tanahair.indonesia.go.id/demnas/#/demnas> (Accessed: January 23, 2021).
- CGIAR (2019) *Global aridity index and potential evapotranspiration (ET<sub>o</sub>) climate database v2*. Figshare. Available at: <https://doi.org/10.6084/m9.figshare.7504448.v3>.
- FAO (2022) *Harmonized world soil database v1.2. FAO SOILS PORTAL*. Rome: Food and Agriculture Organization of the United Nations. Available at: <https://www.fao.org/soils-portal/data-hub/soil-maps-and-databases/harmonized-world-soil-database-v12/en/> (Accessed: January 23, 2022).
- Gan, G., Liu, Y. and Sun, G. (2021) "Understanding interactions among climate, water, and vegetation with the Budyko framework," *Earth-Science Reviews*, 212, 103451. Available at: <https://doi.org/10.1016/j.earscirev.2020.103451>.

- Gerstorff, S. and Schupp, J. (eds.) (2016) *SOEP wave report 2015*. Berlin: SOEP – The German Socio-Economic Panel study at DIW. Available at: [https://www.diw.de/documents/publikationen/73/diw\\_01.c.535678.de/wave\\_report\\_2015.pdf](https://www.diw.de/documents/publikationen/73/diw_01.c.535678.de/wave_report_2015.pdf) (Accessed: January 23, 2022).
- Hamel, P. and Guswa, A.J. (2015) “Uncertainty analysis of a spatially explicit annual water-balance model: case study of the Cape Fear basin, North Carolina,” *Hydrology and Earth System Sciences*, 19(2), pp. 839–853. Available at: <https://doi.org/10.5194/hess-19-839-2015>.
- Liu, W. *et al.* (2017) “Estimations of evapotranspiration in an age sequence of Eucalyptus plantations in subtropical China,” *PLOS ONE*, 12(4), e0174208. Available at: <https://doi.org/10.1371/journal.pone.0174208>.
- Nugroho, N.P. (2022) “Sediment export estimation from the catchment area of Lake Rawapening using InVEST model,” *IOP Conference Series: Earth and Environmental Science*, 950(1), 012072. Available at: <https://doi.org/10.1088/1755-1315/950/1/012072>.
- Sánchez-Canales, M. *et al.* (2012) “Sensitivity analysis of ecosystem service valuation in a Mediterranean watershed,” *Science of The Total Environment*, 440, pp. 140–153. Available at: <https://doi.org/10.1016/j.scitotenv.2012.07.071>.
- Sulaeman, Y. *et al.* (2013) “Harmonizing legacy soil data for digital soil mapping in Indonesia,” *Geoderma*, 192, pp. 77–85. Available at: <https://doi.org/10.1016/j.geoderma.2012.08.005>.
- Tallis, H. *et al.* (2011) *InVEST 2.1 beta user’s guide. The Natural Capital Project, Stanford*. Stanford: Stanford University.